

Half-integer quantized response in strongly driven quantum systems

P. J. D. Crowley,^{1,*} I. Martin,² and A. Chandran¹

¹*Department of Physics, Boston University, Boston, MA 02215, USA*

²*Materials Science Division, Argonne National Laboratory, Argonne, Illinois 60439, USA*

(Dated: August 23, 2019)

A spin strongly driven by two incommensurate tones can pump energy from one drive to the other at a quantized average rate, in close analogy with the quantum Hall effect. The quantized pumping is a pre-thermal effect with a lifetime that diverges as the drive frequencies approach zero. We study the transition between the pumping and non-pumping pre-thermal states. The transition is sharp at zero frequency and is characterized by a Dirac point in the instantaneous band structure parametrized by the drive phases. We show that the pumping rate is *half-integer* quantized at the transition and present universal Kibble-Zurek scaling functions for energy transfer processes in the low frequency regime. Our results identify qubit experiments to measure the universal linear and non-linear response of a Dirac point.

Introduction: A spin driven by a time-dependent magnetic field $\vec{B}(t)$ is a quintessential problem [1–9]. At low drive frequencies ω , the spin’s direction is locked to the instantaneous field direction up to an “unlock time” t_u , after which it effectively heats to infinite temperature.

Recent work has shown that a spin- $\frac{1}{2}$ driven by two circularly polarized magnetic fields with incommensurate frequencies (ω_1 and ω_2) pumps energy from drive 1 to drive 2 at a quantized average rate [10–12]

$$[P_{1T}]_{\vec{\theta}_0} = C_g P_Q \equiv C_g \frac{\omega_1 \omega_2}{2\pi}, \quad (1)$$

where $\hbar = 1$, the spin is prepared in the instantaneous ground state, and C_g equals the Chern number of the instantaneous ground state band as a function of the drive phases. In the trivial regime, $C_g = 0$ and the spin doesn’t pump. In the topological regime however, C_g is a non-zero integer, and the spin pumps energy as long as it is locked to the direction of the field [10, 12]. The lifetime of the pumping is exponentially long in $1/\omega$ in the low-frequency regime and can be further extended by either introducing relaxation processes [11], or by counter-diabatic driving [12–14].

In this letter, we show that C_g , and thus the power, is quantized to a half-integer *at the dynamical transition between the topological and trivial regimes*. The transition is controlled by a sign change of the mass at a Dirac point in the instantaneous band structure [12, 15–17]. However, for times $t \ll t_u$, the spin trajectory is generally far from the Dirac point and the pumping rate is set by the integrated Berry curvature of the ground state band *excluding the Dirac point*.

The half-integer quantized pumping is nontrivial to observe as (i) the spin exchanges energy with the drives when it unlocks, and (ii) an unlocked spin pumps energy at a rate less than in Eq. (1). The unlock time t_u at the transition follows from Kibble-Zurek arguments [18–30],

$$t_u \sim \sqrt{B_0/\omega^3}, \quad (2)$$

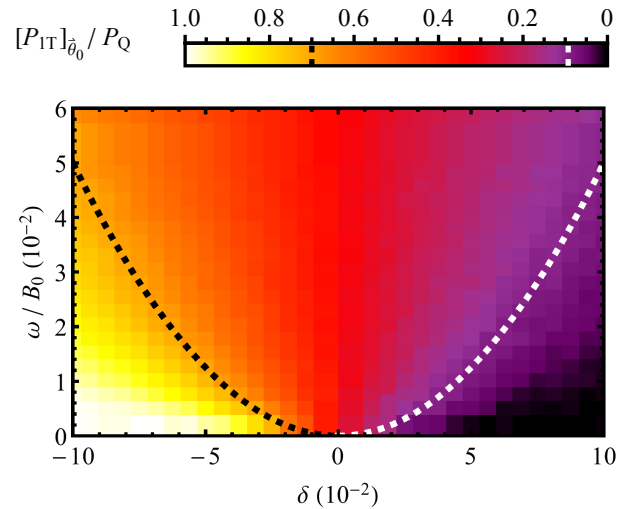


FIG. 1. Density plot of the topological contribution to the pump power $[P_{1T}]_{\vec{\theta}_0}$ as $t/t_u \rightarrow 0$ for the half-BHZ model (Eq. (4)). As $\omega \rightarrow 0$, the power approaches zero in the trivial phase ($\delta > 0$), P_Q in the topological phase ($\delta < 0$) and $P_Q/2$ at the transition ($\delta = 0$). At small finite ω in the Kibble-Zurek scaling limit, the power smoothly crosses over from 0 to P_Q with parabolic level sets (dashed lines).

where B_0 is the typical scale of the magnetic field acting on the spin.

We show that the average power has two universal contributions as $t/t_u \rightarrow 0$: [31]

$$[P_1]_{\vec{\theta}_0} = \frac{1}{2} P_Q + \frac{B_0}{t_u}. \quad (3)$$

The second term, due to spin excitation, dominates the topological term as $\omega \rightarrow 0$. However, drawing intuition from the action of time-reversal on Chern insulators, we isolate the topological and excitation terms and their associated *universal Kibble-Zurek scaling functions* using time evolution with the Hamiltonian and its complex conjugate (see Fig. 1). Experimentally, complex conjugation corresponds to reversing the circular polarization of one

* philip.jd.crowley@gmail.com

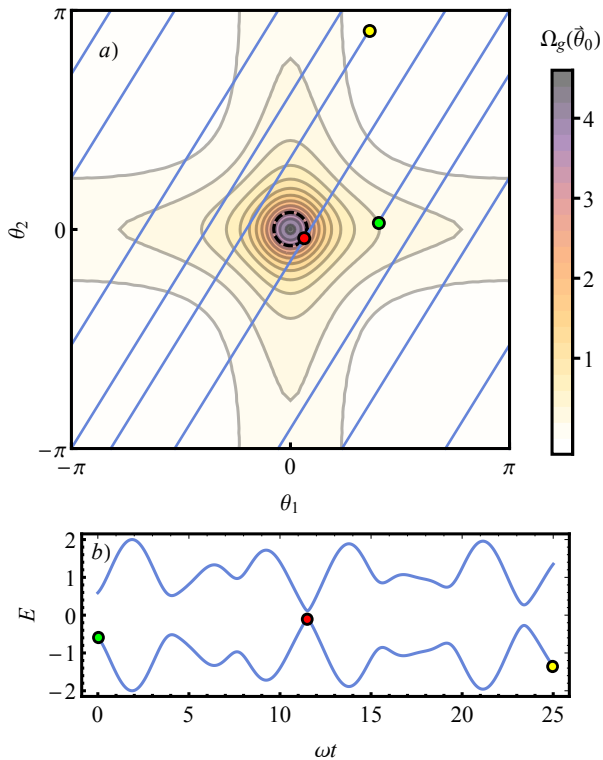


FIG. 2. Upper plot: Contour plot of the Berry curvature of the instantaneous ground state near to the transition ($\delta = -1/3$). The drive phase trajectory (blue lines) starting from $\vec{\theta}_0$ (green point). The integrated Berry curvature sets the (average) pumping rate until the spin enters the excitation region $|\vec{\theta}_t| < \theta^*$ (dashed circle) for the first time (red point). At this point, the spectral gap of $H(\vec{\theta}_t)$ is too small to maintain adiabaticity (lower plot), the spin unlocks, and the pumping rate decreases.

of the drives. Incommensurately driven few-level quantum systems thus offer a unique window into the universal properties of the topological phase transitions of band insulators.

Model: For concreteness, we work with the same “half-BHZ model” as Refs. [10–12]. The Hamiltonian is

$$\begin{aligned} H(\vec{\theta}_t) &= -\frac{1}{2}\vec{B}(\vec{\theta}_t) \cdot \vec{\sigma} \\ \vec{B}(\vec{\theta}_t) &= B_0(\sin \theta_{t1}, \sin \theta_{t2}, 2 + \delta - \cos \theta_{t1} - \cos \theta_{t2}), \end{aligned} \quad (4)$$

where $\vec{\theta}_t = (\theta_{t1}, \theta_{t2})$ is the vector of drive phases, $\theta_{ti} = \omega_i t + \theta_{0i}$ for $i = 1, 2$ and the ratio of the drive frequencies ω_2/ω_1 is an irrational number. We assume that the ratio of drive frequencies is order one, so that $\omega = \sqrt{\omega_1\omega_2}$ is the single frequency-scale on which H varies. The spin is prepared in the instantaneous ground state at $t = 0$.

Instantaneous band structure: The instantaneous band structure consists of bands with energies $\pm \frac{1}{2}|\vec{B}(\vec{\theta})|$ over the torus $\vec{\theta} \in [0, 2\pi)^2$. At each $\vec{\theta}$, the spin in the ground (excited) band is aligned (anti-aligned) with $\vec{B}(\vec{\theta})$. This band structure is identical to that of the half-BHZ model

in momentum space [15, 32, 33]. The ground state band has Chern number $C_g = 1$ for $-2 < \delta < 0$, and $C_g = 0$ for $\delta > 0$.

In the vicinity of the transition at $\delta = 0$, there is a massive Dirac point in the band structure at $|\vec{\theta}| = 0$:

$$H(\vec{\theta}) = -\frac{B_0}{2}(\theta_1\sigma_x + \theta_2\sigma_y + \delta\sigma_z) + O(|\vec{\theta}|^2). \quad (5)$$

Fig. 2a is a density plot of the Berry curvature of the ground state band in the topological regime, close to the transition. The Berry curvature has two contributions: a piece that is smooth in δ and $\vec{\theta}$ and integrates to π ; and a singular piece which concentrates into a delta function at $\vec{\theta} = \vec{0}$ and integrates to $-\text{sgn}(\delta)\pi$ [15, 32].

The drive phases follow trajectories of constant slope in $\vec{\theta}$ -space (shown in blue in Fig. 2a). Consider $t \ll t_u$. Away from the Dirac point, the Berry curvature is small, and the spin state along the trajectory approximately follows the instantaneous ground state [34]. In the low frequency limit and with ω_2/ω_1 irrational, the trajectory uniformly samples this Berry curvature over time.

We show below that the average power is set by the integrated Berry curvature of the instantaneous ground state band *before unlock*. Sufficiently far away from the transition, the trajectory samples the entire Berry curvature. At the transition, however, the spin unlocks before sampling the singular component associated with the Dirac point. Thus, the integrated Berry curvature in Eq. (1) is given by

$$C_g = \begin{cases} 1 & \delta < 0 \\ \frac{1}{2} & \delta = 0 \\ 0 & \delta > 0. \end{cases} \quad (6)$$

Pump power: The instantaneous rate of energy transfer from drive 1 is given by [10]

$$P_1 \equiv \omega_1 \langle \partial_{\theta_1} H \rangle, \quad (7)$$

with a corresponding expression for P_2 . As the spin cannot absorb energy indefinitely, the net energy flux into the system time-averages to zero, $[P_{\text{tot}}]_t = [P_1]_t + [P_2]_t = 0$. Throughout, $[\cdot]_x$ denotes averaging with respect to variable x .

In the low frequency limit, P_1 is a sum of two terms, one analytic and one non-analytic in ω . The analytic term is completely determined by the instantaneous values of $\vec{\theta}_t$, while the non-analytic terms depend on the entire history of the trajectory. As in the Landau-Zener problem, the analytic terms describe the perturbative “dressing” of the spin state over the instantaneous ground state [34–36]. The non-analytic terms capture the non-adiabatic excitation processes between the dressed states. Below we refer to the leading order analytic term as P_{1T} , as it is of topological origin, and non-analytic term as P_{1E} , which is due to excitations.

Topological contribution to pumping for $t \ll t_u$: We now derive Eq. (1) with C_g given by Eq. (6). Let $|\tilde{g}(\vec{\theta}_t)\rangle$

be the spin state dressed to order ω above the instantaneous ground state. Thus,

$$\begin{aligned} i\frac{d|\tilde{g}\rangle}{dt} &= H|\tilde{g}\rangle + O(\omega^2) \\ \Rightarrow H|\tilde{g}\rangle &= i\omega_1|\partial_{\theta_1}\tilde{g}\rangle + i\omega_2|\partial_{\theta_2}\tilde{g}\rangle + O(\omega^2). \end{aligned} \quad (8)$$

where we have suppressed the time dependence of $\vec{\theta}$ for brevity. Using the product rule, we obtain

$$\begin{aligned} P_{1T} &= \omega_1\langle\tilde{g}|\partial_{\theta_1}H|\tilde{g}\rangle \\ &= \omega_1[\partial_{\theta_1}\langle\tilde{g}|H|\tilde{g}\rangle - \langle\partial_{\theta_1}\tilde{g}|H|\tilde{g}\rangle - \langle\tilde{g}|H|\partial_{\theta_1}\tilde{g}\rangle] \\ &= \omega_1\partial_{\theta_1}\langle\tilde{g}|H|\tilde{g}\rangle + \omega_1\omega_2\Omega_{\tilde{g}}(\vec{\theta}), \end{aligned} \quad (9)$$

where $\Omega_{\tilde{g}}(\vec{\theta}) = 2\text{Im}\langle\partial_{\theta_1}\tilde{g}|\partial_{\theta_2}\tilde{g}\rangle$ is the Berry curvature of the dressed spin state.

The instantaneous power varies with the initial phase vector $\vec{\theta}_0$. Universal results about the spin dynamics at each t follow upon initial phase averaging

$$\begin{aligned} [P_{1T}]_{\vec{\theta}_0} &= [\partial_{\theta_{1t}}\langle\tilde{g}|H|\tilde{g}\rangle]_{\vec{\theta}_0} + \omega_1\omega_2[\Omega_{\tilde{g}}(\vec{\theta}_t)]_{\vec{\theta}_0} \\ &= C_g P_Q. \end{aligned} \quad (10)$$

The first term vanishes as it is a total derivative. The second term is the integrated Berry curvature of the dressed band prior to unlock (and thus excludes the Dirac point). As the integrated Berry curvature of the dressed and instantaneous bands are identical, we obtain Eq. (1).

Kibble-Zurek estimate for t_u : The probability to transition to the dressed instantaneous excited state follows from the Landau-Zener result [36–39]

$$p_{\text{exc}} \sim \max_t \exp\left(-\frac{\pi|\vec{B}(\vec{\theta}_t)|^2}{|\partial_t\vec{B}|}\right). \quad (11)$$

Deep in the topological or trivial regimes, the spin's evolution thus remains adiabatic for an exponentially long time-scale $\sim \exp(B_0/\omega)$.

Eq. (11) predicts that the spin unlocks from the field when the instantaneous gap squared becomes comparable or smaller than the rate of change of the field [18–22, 24, 27–29]. At the transition, the spin thus unlocks when

$$|\vec{\theta}_t| \lesssim \theta^* = \sqrt{\omega/B_0}. \quad (12)$$

This relation defines the ‘‘excitation region’’ within the dashed circle in Fig. 2a. A typical spin trajectory enters the excitation region for the first time after $2\pi/\theta^*$ periods. We thus obtain the scaling of the unlock time $t_u \sim (\omega\theta^*)^{-1} \sim \sqrt{B_0/\omega^3}$ previously stated in Eq. (2).

In the vicinity of the transition, the spin trajectory encounters small gaps of order $B_0\delta$ near $\vec{\theta} = \vec{0}$ (Fig. 2b). If the frequency is sufficiently small

$$\omega < \omega^* \sim B_0\delta^2, \quad (13)$$

then the dynamics is adiabatic through the small gaps. The pumped power for $t \ll t_u$ is then set by the $\omega \rightarrow 0$ ‘phases’. However, when $\omega > \omega^*$, the transition controls the spin dynamics. The parabola in Fig. 1 separates these two regimes and defines the critical ‘fan’.

Topological contribution to pumping for $t \gg t_u$: At times much longer than the unlock time, non-adiabatic processes heat the spin. In the initial phase ensemble, the populations in the (dressed) instantaneous ground and excited states thus become equal. As the Chern numbers of the ground and excited state bands sum to zero, the ensemble averaged power $[P_{1T}]_{\vec{\theta}_0} \rightarrow 0$ as $t/t_u \rightarrow \infty$.

Excitation contribution to pumping: The non-adiabatic excitation of the spin results in a distinct contribution to the power $[P_{1E}]_{\vec{\theta}_0}$. As the spin absorbs order B_0 energy from the drives over a time-scale t_u

$$[P_{1E}]_{\vec{\theta}_0} \sim B_0/t_u \propto \omega^{3/2}, \quad t \lesssim t_u. \quad (14)$$

Unlike the topological contribution, the power due to excitation is non-analytic in ω . The total pumped power is the sum of the topological and excitation contributions. Using Eqs. (10) and (14), we obtain the result Eq. (3) quoted in the introduction.

A constant rate of excitation results in a linear increase of the excited state population in the initial phase ensemble at small t/t_u . At late times, the populations become equal, and statistically the spin ceases to absorb energy from the drives. Thus, $[P_{1E}]_{\vec{\theta}_0} \rightarrow 0$ as $t/t_u \rightarrow \infty$.

Kibble-Zurek scaling functions: Within the Kibble-Zurek (KZ) scaling limit, the non-equilibrium dynamics of the spin becomes universal even beyond the unlock time. The KZ scaling limit involves taking $\omega, \delta \rightarrow 0$ which measuring time in units of the diverging unlock time t_u , and the drive frequency in units of the vanishing scale ω^* [20, 23, 25–29]. In this limit, the radius of the excitation region θ^* becomes small and the Hamiltonian of the massive Dirac cone (Eq. (5)) controls the excitation of the spin, and hence the decay of the topological component of the power. The topological and excitation components of the power then take the following scaling forms

$$\begin{aligned} [P_{1E}(t; \omega, \delta)]_{\vec{\theta}_0} &\sim \omega^{3/2}\mathcal{P}_{1E}(t\omega^{3/2}; \delta\omega^{-1/2}), \\ [P_{1T}(t; \omega, \delta)]_{\vec{\theta}_0} &\sim \frac{\omega^2}{2\pi}\mathcal{P}_{1T}(t\omega^{3/2}; \delta\omega^{-1/2}). \end{aligned} \quad (15)$$

Above, \mathcal{P}_{1E} and \mathcal{P}_{1T} are scaling functions determined solely by the universality class of the transition in the instantaneous band structure. They capture the universal cross-over from the pre-thermal regime to the late-time infinite-temperature regime.

Scaling functions for the Dirac transition: We now numerically extract the scaling forms $\mathcal{P}_{1E}, \mathcal{P}_{1T}$ for the Dirac transition in the half-BHZ model using complex-conjugation of the Hamiltonian $H'(\vec{\theta}_t) = (H(\vec{\theta}_t))^*$. Physically, this is achieved by flipping the chirality of the circular polarization of drive 2. The Supplemental Material obtains the same scaling functions for a different microscopic model with a Dirac transition, demonstrating universality.

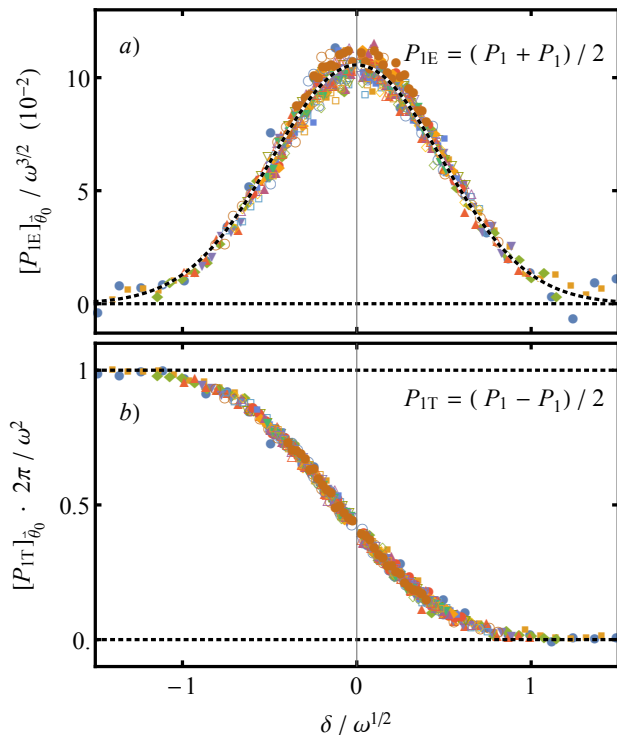


FIG. 3. The phase-averaged excitation (top) and topological (bottom) scaling functions of the power at $t\omega^{3/2} = 1.72$ ($t/t_u \approx 0.3$). As $p_{\text{exc}} \propto \mathcal{P}_{1E}$, the top panel is fit well by a Gaussian. The topological scaling function decreases from one deep in the topological phase $\delta \ll -\omega^{1/2}$, to approximately one-half at the transition at $\delta = 0$ and to zero in the trivial phase. Parameters: $B_0 = 1$, ω_2/ω_1 is the golden ratio and 20 values of $\omega \in [0.0025, 0.1]$.

In the scaling limit, the following relations hold

$$\begin{aligned} [P_{1E}]_{\vec{\theta}_0} &= \frac{1}{2} \left([P_1]_{\vec{\theta}_0} + [P'_1]_{\vec{\theta}_0} \right) \\ [P_{1T}]_{\vec{\theta}_0} &= \frac{1}{2} \left([P_1]_{\vec{\theta}_0} - [P'_1]_{\vec{\theta}_0} \right), \end{aligned} \quad (16)$$

where $P'_1 = \omega_1 \langle \psi'_t | \partial_{\theta_1} H'(\vec{\theta}_t) | \psi'_t \rangle$, the conjugated system $i\partial_t |\psi'_t\rangle = H'(\vec{\theta}_t) |\psi'_t\rangle$ is initialized in its instantaneous ground-state band $|\psi'_0\rangle = (|\psi_0\rangle)^*$.

Eq. (16) is obtained as follows. As the probability of excitation in Eq. (11) is invariant under complex conjugation, the ensemble populations of the instantaneous eigenstates are the same at each t/t_u for time evolution under H and H' . Thus, $[P'_{1E}]_{\vec{\theta}_0} = [P_{1E}]_{\vec{\theta}_0}$. The topological piece however changes sign, $[P'_{1T}]_{\vec{\theta}_0} = -[P_{1T}]_{\vec{\theta}_0}$ as the Berry curvature changes sign under complex conjugation.

Fig. 3 shows the scaling functions across the transition for both contributions as a function $\delta/\omega^{1/2}$ for small t/t_u . They confirm the scaling collapse of the (two-dimensional) data from Fig. 1. The excitation scaling function is proportional to excitation probability for $t \ll t_u$. As $p_{\text{exc}} \sim \exp(-\delta^2 B_0/\omega)$, Fig. 3a is thus well fit by a Gaussian centred at the transition (black-white

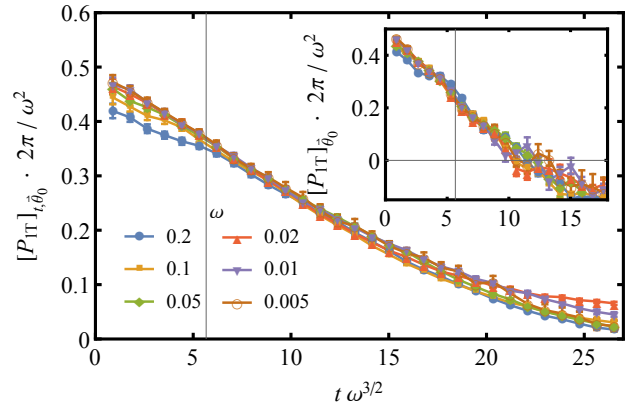


FIG. 4. The topological scaling function at the transition with (main) and without time-averaging (inset). Both plots show that the scaling function approaches $1/2$ as $t\omega^{3/2} \rightarrow 0$, and zero as $t\omega^{3/2} \rightarrow \infty$. The vertical line is a proxy for t_u (definition in text).

dashed line).

Fig. 3b shows that $[P_{1T}]/P_Q$ obeys a single-parameter scaling function at fixed t/t_u , with the limiting values of one/zero as $\delta \rightarrow \mp\infty$ (Eq. (6)). The intermediate value at $\delta = 0$ is close to $\frac{1}{2}$, and approaches it as $t/t_u \rightarrow 0$. At non-zero $\delta/\omega^{1/2}$, the component of the Berry curvature that is singular at the transition has a width comparable to that of the excitation region θ^* . Consequently, this component is partially sampled by spin trajectories before unlock and leads to the smooth universal function observed in Fig. 3b. Note Eq. (6) is contained within the scaling function in Eq. (15) on taking $\omega \rightarrow 0$ at fixed δ .

A technical comment: the data in Fig. 3 is time-averaged over $t\omega^{3/2}$ within the interval $[0, 1.72]$ (in addition to initial phase averaged). This reduces fluctuations due to the sampling of $\vec{\theta}_0$ and slightly modifies the value of the scaling function near $\delta = 0$.

We now turn to the dependence of the scaling functions on t/t_u . Fig. 4 (inset) shows $\mathcal{P}_{1T} \sim [P_{1T}]_{\vec{\theta}_0}/P_Q$ at the transition, whilst the main figure shows the power with additional averaging over the time interval $[0, t]$. The gray vertical line is a proxy for t_u and identifies the mean time up to which $|\partial_t \vec{B}| < |\vec{B}|^2$. Both plots show that \mathcal{P}_{1T} approaches the quantized value of $1/2$ only as $t/t_u \rightarrow 0$. Next, for $0 < t/t_u \ll 1$, \mathcal{P}_{1T} linearly decreases. This linear decrease follows from the constant excitation rate in Eq. (14) and the opposite sign of the pumping by the excited population. Finally, despite the negative turn at $t\omega^{3/2} \approx 10$ in the inset, we find that \mathcal{P}_{1T} approaches zero for $t/t_u \gg 1$, consistent with the main figure.

Discussion: We have demonstrated that a simple quasiperiodically driven spin- $\frac{1}{2}$ exhibits universal scaling behaviors characteristic of extended classical or quantum *equilibrium* systems in the vicinity of continuous phase transitions [40, 41]. Our results serve as a new example of the tantalising correspondence emerging between equilibrium systems and systems subject to periodic or

quasi-periodic driving [10–12, 42–78].

The KZ scaling functions also provide the universal non-linear response of a clean Dirac material in an electric field [79]. On Fourier transforming the $\vec{\theta}$ coordinates, the model in Eq. (4) is equivalent to the real-space half-BHZ model with an additional electric field (ω_1, ω_2) [10, 12]. If we identify ω with the magnitude of the electric field, then the topological component of the power is the Hall response, while the excitation component measures the population in the excited band due to dielectric breakdown when the insulator is initially at zero temperature.

Driven few-level systems can access other topological phase transitions in static systems using different driv-

ing protocols. Moreover, the KZ scaling theory can be extended to include the effects of dissipation [11], or counter-diabatic driving [12]. Both effects increase the unlock time t_u , and may simplify experimental access to the half-quantized response in solid-state and quantum optical platforms that host qubits [4–9, 80–88].

Acknowledgements: We are grateful to E. Boyers, W.W. Ho, C. R. Laumann, D. Long, A. Polkovnikov, D. Sels and A. Sushkov for useful discussions. This work was supported by NSF DMR-1752759 (P.C. and A.C.), and completed at the Aspen Center for Physics, which is supported by the NSF grant PHY-1607611. A.C. acknowledges support from the Sloan Foundation through the Sloan Research Fellowship. Work at Argonne was supported by the Department of Energy, Office of Science, Materials Science and Engineering Division.

-
- [1] M. H. Levitt, *Spin dynamics: basics of nuclear magnetic resonance* (John Wiley & Sons, 2001).
- [2] M. A. Nielsen and I. Chuang, “Quantum computation and quantum information,” (2002).
- [3] G. K. Woodgate, *Elementary Atomic Structure* (Oxford University Press, 1970).
- [4] I. Buluta, S. Ashhab, and F. Nori, Reports on Progress in Physics **74**, 104401 (2011).
- [5] J. Clarke and F. K. Wilhelm, Nature **453**, 1031 (2008).
- [6] V. Dobrovitski, G. Fuchs, A. Falk, C. Santori, and D. Awschalom, Annu. Rev. Condens. Matter Phys. **4**, 23 (2013).
- [7] C. Kloeffer and D. Loss, Annu. Rev. Condens. Matter Phys. **4**, 51 (2013).
- [8] H. Häffner, C. F. Roos, and R. Blatt, Physics reports **469**, 155 (2008).
- [9] M. H. Devoret, A. Wallraff, and J. M. Martinis, arXiv preprint cond-mat/0411174 (2004).
- [10] I. Martin, G. Refael, and B. Halperin, Physical Review X **7**, 041008 (2017).
- [11] F. Nathan, I. Martin, and G. Refael, Physical Review B **99**, 094311 (2019).
- [12] P. J. Crowley, I. Martin, and A. Chandran, Physical Review B **99**, 064306 (2019).
- [13] A. del Campo, Physical review letters **111**, 100502 (2013).
- [14] D. Sels and A. Polkovnikov, Proceedings of the National Academy of Sciences , 201619826 (2017).
- [15] B. A. Bernevig and T. L. Hughes, *Topological insulators and topological superconductors* (Princeton university press, 2013).
- [16] M. Z. Hasan and C. L. Kane, Reviews of Modern Physics **82**, 3045 (2010).
- [17] A. Bansil, H. Lin, and T. Das, Reviews of Modern Physics **88**, 021004 (2016).
- [18] T. W. Kibble, Journal of Physics A: Mathematical and General **9**, 1387 (1976).
- [19] W. H. Zurek, Nature **317**, 505 (1985).
- [20] A. Polkovnikov, Physical Review B **72**, 161201 (2005).
- [21] W. H. Zurek, U. Dorner, and P. Zoller, Physical review letters **95**, 105701 (2005).
- [22] J. Dziarmaga, Physical review letters **95**, 245701 (2005).
- [23] S. Deng, G. Ortiz, and L. Viola, EPL (Europhysics Letters) **84**, 67008 (2009).
- [24] J. Dziarmaga, Advances in Physics **59**, 1063 (2010).
- [25] G. Biroli, L. F. Cugliandolo, and A. Sicilia, Physical Review E **81**, 050101 (2010).
- [26] C. De Grandi, A. Polkovnikov, and A. Sandvik, Physical Review B **84**, 224303 (2011).
- [27] A. Polkovnikov and V. Gritsev, Understanding Quantum Phase Transitions , 59 (2011).
- [28] A. Chandran, A. Erez, S. S. Gubser, and S. L. Sondhi, Physical Review B **86**, 064304 (2012).
- [29] M. Kolodrubetz, B. K. Clark, and D. A. Huse, Physical review letters **109**, 015701 (2012).
- [30] A. D. Campo and W. H. Zurek, in *Symmetry and Fundamental Physics: Tom Kibble at 80* (World Scientific, 2014) pp. 31–87.
- [31] Here the $\frac{1}{2}$ indicates a transition between abutting $C_g = 1, 0$ phases.
- [32] X.-L. Qi, Y.-S. Wu, and S.-C. Zhang, Physical Review B **74**, 085308 (2006).
- [33] B. A. Bernevig, T. L. Hughes, and S.-C. Zhang, Science **314**, 1757 (2006).
- [34] P. Weinberg, M. Bukov, L. D’Alessio, A. Polkovnikov, S. Vajna, and M. Kolodrubetz, Physics Reports **688**, 1 (2017).
- [35] G. Rigolin, G. Ortiz, and V. H. Ponce, Physical Review A **78**, 052508 (2008).
- [36] C. De Grandi and A. Polkovnikov, in *Quantum Quenching, Annealing and Computation* (Springer, 2010) pp. 75–114.
- [37] C. Zener, Proc. R. Soc. Lond. A **137**, 696 (1932).
- [38] L. D. Landau, Ukr. J. Phys. **11**, 19 (1937).
- [39] L. Landau, Phys. Z. Sowjetunion **11**, 26 (1937).
- [40] J. Cardy, *Scaling and renormalization in statistical physics*, Vol. 5 (Cambridge university press, 1996).
- [41] S. Sachdev, Physics world **12**, 33 (1999).
- [42] T.-S. Ho, S.-I. Chu, and J. V. Tietz, Chemical Physics Letters **96**, 464 (1983).
- [43] J. Luck, H. Orland, and U. Smilansky, Journal of statistical physics **53**, 551 (1988).
- [44] H. Jauslin and J. Lebowitz, Chaos: An Interdisciplinary Journal of Nonlinear Science **1**, 114 (1991).

- [45] P. Blekher, H. Jauslin, and J. Lebowitz, *Journal of statistical physics* **68**, 271 (1992).
- [46] H. Jauslin and J. Lebowitz, in *Mathematical Physics X* (Springer, 1992) pp. 313–316.
- [47] T. Kitagawa, T. Oka, A. Brataas, L. Fu, and E. Demler, *Physical Review B* **84**, 235108 (2011).
- [48] N. H. Lindner, G. Refael, and V. Galitski, *Nature Physics* **7**, 490 (2011).
- [49] L. Jiang, T. Kitagawa, J. Alicea, A. Akhmerov, D. Pekker, G. Refael, J. I. Cirac, E. Demler, M. D. Lukin, and P. Zoller, *Physical review letters* **106**, 220402 (2011).
- [50] J. Cayssol, B. Dóra, F. Simon, and R. Moessner, *physica status solidi (RRL)-Rapid Research Letters* **7**, 101 (2013).
- [51] Y. T. Katan and D. Podolsky, *Physical review letters* **110**, 016802 (2013).
- [52] M. S. Rudner, N. H. Lindner, E. Berg, and M. Levin, *Physical Review X* **3**, 031005 (2013).
- [53] T. Iadecola, D. Campbell, C. Chamon, C.-Y. Hou, R. Jackiw, S.-Y. Pi, and S. V. Kusminskiy, *Physical review letters* **110**, 176603 (2013).
- [54] P. Delplace, Á. Gómez-León, and G. Platero, *Physical Review B* **88**, 245422 (2013).
- [55] A. Kundu, H. Fertig, and B. Seradjeh, *Physical review letters* **113**, 236803 (2014).
- [56] A. G. Grushin, Á. Gómez-León, and T. Neupert, *Physical review letters* **112**, 156801 (2014).
- [57] M. Lababidi, I. I. Satija, and E. Zhao, *Physical review letters* **112**, 026805 (2014).
- [58] A. Chandran and S. L. Sondhi, *Physical Review B* **93**, 174305 (2016).
- [59] A. Verdeny, J. Puig, and F. Mintert, *Zeitschrift für Naturforschung A* **71**, 897 (2016).
- [60] V. Khemani, A. Lazarides, R. Moessner, and S. L. Sondhi, *Physical review letters* **116**, 250401 (2016).
- [61] C. W. von Keyserlingk and S. L. Sondhi, *Physical Review B* **93**, 245145 (2016).
- [62] C. W. von Keyserlingk and S. L. Sondhi, *Physical Review B* **93**, 245146 (2016).
- [63] R. Roy and F. Harper, *Physical Review B* **94**, 125105 (2016).
- [64] D. V. Else and C. Nayak, *Physical Review B* **93**, 201103 (2016).
- [65] F. Nathan, M. S. Rudner, N. H. Lindner, E. Berg, and G. Refael, *Physical review letters* **119**, 186801 (2017).
- [66] R. Roy and F. Harper, *Physical Review B* **96**, 155118 (2017).
- [67] R. Moessner and S. Sondhi, *Nature Physics* **13**, 424 (2017).
- [68] Y. Baum and G. Refael, *Physical review letters* **120**, 106402 (2018).
- [69] Y. Peng and G. Refael, *Physical Review B* **97**, 134303 (2018).
- [70] I. Mondragon-Shem, I. Martin, A. Alexandradinata, and M. Cheng, *arXiv preprint arXiv:1811.10632* (2018).
- [71] M. H. Kolodrubetz, F. Nathan, S. Gazit, T. Morimoto, and J. E. Moore, *Physical review letters* **120**, 150601 (2018).
- [72] P. T. Dumitrescu, R. Vasseur, and A. C. Potter, *Physical review letters* **120**, 070602 (2018).
- [73] Y. Peng and G. Refael, *Physical Review B* **98**, 220509 (2018).
- [74] Y. Peng and G. Refael, *Physical Review Letters* **123**, 016806 (2019).
- [75] B. Bauer, T. Pereg-Barnea, T. Karzig, M.-T. Rieder, G. Refael, E. Berg, and Y. Oreg, *Physical Review B* **100**, 041102 (2019).
- [76] T. Ozawa and H. M. Price, *Nature Reviews Physics* , 1 (2019).
- [77] H. Hu, B. Huang, E. Zhao, and W. V. Liu, *arXiv preprint arXiv:1905.03727* (2019).
- [78] T. Oka and S. Kitamura, *Annual Review of Condensed Matter Physics* **10**, 387 (2019).
- [79] A. G. Green and S. L. Sondhi, *Physical review letters* **95**, 267001 (2005).
- [80] F. Jelezko, T. Gaebel, I. Popa, M. Domhan, A. Gruber, and J. Wrachtrup, *Physical Review Letters* **93**, 130501 (2004).
- [81] C. Langer, R. Ozeri, J. D. Jost, J. Chiaverini, B. DeMarco, A. Ben-Kish, R. Blakestad, J. Britton, D. Hume, W. M. Itano, *et al.*, *Physical review letters* **95**, 060502 (2005).
- [82] J. Taylor, H.-A. Engel, W. Dür, A. Yacoby, C. Marcus, P. Zoller, and M. Lukin, *Nature Physics* **1**, 177 (2005).
- [83] B. Trauzettel, D. V. Bulaev, D. Loss, and G. Burkard, *Nature Physics* **3**, 192 (2007).
- [84] A. Gali, *Physical Review B* **79**, 235210 (2009).
- [85] R. Blatt and C. F. Roos, *Nature Physics* **8**, 277 (2012).
- [86] T. Harty, D. Allcock, C. J. Ballance, L. Guidoni, H. Janacek, N. Linke, D. Stacey, and D. Lucas, *Physical review letters* **113**, 220501 (2014).
- [87] G. Wendin, *Reports on Progress in Physics* **80**, 106001 (2017).
- [88] Y. Wang, M. Um, J. Zhang, S. An, M. Lyu, J.-N. Zhang, L.-M. Duan, D. Yum, and K. Kim, *Nature Photonics* **11**, 646 (2017).

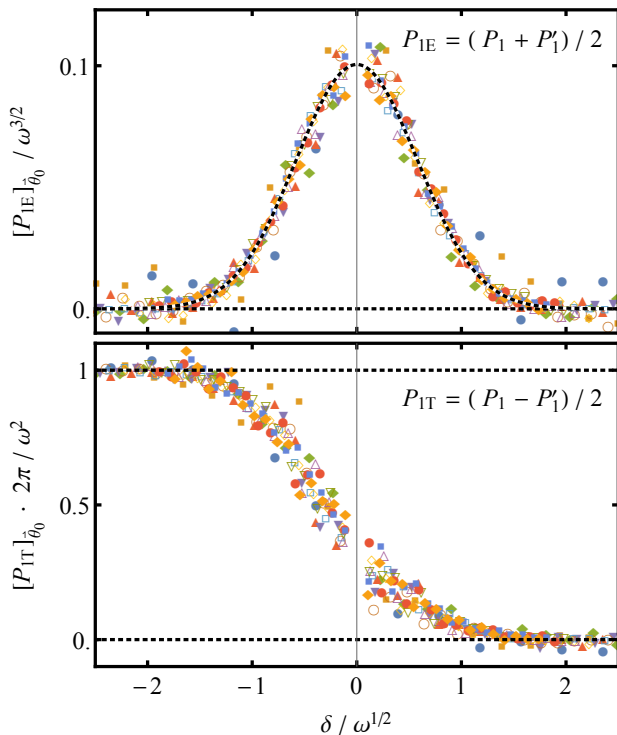


FIG. 5. The phase-averaged excitation (top) and topological (bottom) scaling functions of the power at $t\omega^{3/2} = 3.43$. In re-scaled units, the scaling functions are identical to those in Fig. 3. Parameters: \vec{B} given by (21) with $(n_1, n_2) = (1, 3)$ and $\phi = 4\pi/5$, $B_0 = 1$, ω_2/ω_1 is the golden ratio and we use 13 values of $\omega \in [1.6 \times 10^{-4}, 3 \times 10^{-2}]$.

SUPPLEMENTAL INFORMATION

Universality of scaling functions at the Dirac transition

The Hamiltonian used in the main text (Eq. (4)) is a well known model [15–17, 32], which has several special symmetries. Universality requires that the scaling functions $\mathcal{P}_{1E}, \mathcal{P}_{1T}$ do not depend on these symmetries. Here we repeat the numerical analysis shown in the main text using a model which lacks these symmetries. We obtain scaling collapse in the KZ scaling limit and identical

scaling functions to that in Fig. 5.

Symmetries of the Hamiltonian (4) relate non-trivial actions in $\vec{\theta}$ -space to rotations of the spin:

$$\begin{aligned} H(-\vec{\theta}) &= \sigma_z H(\vec{\theta}) \sigma_z \\ -(H(\vec{\theta}))^* &= \sigma_y H(\vec{\theta}) \sigma_y \\ H(\theta_2, -\theta_1) &= U_{\pi/2} H(\theta_1, \theta_2) U_{\pi/2}^\dagger. \end{aligned} \quad (17)$$

Here $U_\phi = \exp(-i\phi\sigma_z/2)$. Furthermore, in the vicinity of the Dirac point at $\delta = 0$,

$$H(\vec{\theta}) = -\frac{B_0}{2} \begin{pmatrix} \theta_1 \\ \theta_2 \\ 0 \end{pmatrix} \cdot \vec{\sigma} - \frac{B_0}{4} \begin{pmatrix} 0 \\ 0 \\ |\vec{\theta}|^2 \end{pmatrix} \cdot \vec{\sigma} + O(|\vec{\theta}_t|^3), \quad (18)$$

and the final relation in Eq. (17) holds for any rotation angle

$$H(R_\phi \vec{\theta}_t) = U_\phi H(\vec{\theta}_t) U_\phi^\dagger + O(|\vec{\theta}_t|^3). \quad (19)$$

Above R_ϕ is a rotation by angle ϕ in $\vec{\theta}$ -space

$$R_\phi = \begin{pmatrix} \cos \phi & -\sin \phi \\ \sin \phi & \cos \phi \end{pmatrix}. \quad (20)$$

To break the symmetries in Eq. (17), consider a spin- $\frac{1}{2}$ driven by the magnetic field $\vec{B}(\vec{\theta}_t)$

$$\vec{B}(\vec{\theta}) = B_0 \begin{pmatrix} \sin(n_1\theta_1 - \phi) + \sin \phi \\ \sin(n_2\theta_2 - \phi) + \sin \phi \\ 2 + \delta - \cos \theta_1 - \cos \theta_2 \end{pmatrix}. \quad (21)$$

For $\cos \phi \neq 0$, $n_1 \neq n_2$ there is an asymmetric Dirac point at $\delta = 0, \vec{\theta} = \vec{0}$,

$$\begin{aligned} H(\vec{\theta}) &= -\frac{B_0 \cos \phi}{2} \begin{pmatrix} n_1\theta_1 \\ n_2\theta_2 \\ 0 \end{pmatrix} \cdot \vec{\sigma} - \frac{B_0}{4} \begin{pmatrix} n_1^2\theta_1^2 \sin \phi \\ n_2^2\theta_2^2 \sin \phi \\ |\vec{\theta}|^2 \end{pmatrix} \cdot \vec{\sigma} \\ &\quad + O(|\vec{\theta}|^3). \end{aligned} \quad (22)$$

Fig 5 shows the scaling collapse obtained for the topological and trivial contributions to the power. In rescaled units, the scaling functions are identical to those obtained in the main text (Fig 3).